JOURNAL OF VIROLOGY, Aug. 1994, p. 4879–4889
0022-538X/94/$04.00+0

Vol. 68, No. 8

Incorporation of Homologous and Heterologous Proteins into the Envelope of Moloney Murine Leukemia Virus

MAARIT SUOMALAINEN* AND HENRIK GAROFF

Department of Molecular Biology, Karolinska Institute, Novum, S-141 57 Huddinge, Sweden

Received 23 February 1994/Accepted 20 April 1994

The efficiencies with which homologous and heterologous proteins are incorporated into the envelope of Moloney murine leukemia virus (M-MuLV) have been analyzed by utilizing a heterologous, Semliki Forest virus-driven M-MuLV assembly system and quantitative pulse-chase assays. Homologous M-MuLV spike protein was found to be efficiently incorporated into extracellular virus particles when expressed at a relatively low density at the plasma membrane. In contrast, efficient incorporation of heterologous proteins (the spike complex of Semliki Forest virus and a cytoplasmically truncated mutant of the human transferrin receptor) was observed only when these proteins were expressed at high densities at the cell surface. These results imply that homologous and heterologous proteins are incorporated into the M-MuLV envelope via two distinct pathways.

Retroviruses mature by budding at the plasma membrane. Recent studies have indicated that the actual budding process is driven by the viral core component, i.e., the Gag precursor, since retroviral Gag precursors expressed in the absence of other viral components were found to be capable of assembling into noninfectious virion-like particles (12, 21, 22, 44, 47). However, formation of infectious retroviral particles requires that not only Gag precursors but also the viral genome, Gag-Pol precursors, and viral spike proteins must all colocalize to the budding site. A considerable amount of data suggests that the viral genome and Gag-Pol precursors are included into budding structures via specific interactions of these components with Gag precursors (30, 38, 46, 49). In contrast, it is unclear at present whether specific core-spike interactions direct incorporation of viral spike proteins into virions. It has been demonstrated that mutations in the matrix domain of the HIV-1 or the Mason-Pfizer monkey virus Gag precursor can impair inclusion of the respective viral spike proteins into virions (14, 43, 60), thereby strongly suggesting that core-spike interactions are needed for incorporation of spikes into virions. However, there is evidence that heterologous proteins, which are apparently unrelated to the homologous spike proteins, can be incorporated into retroviral envelopes. For example, coinfection of cells with a retrovirus and an unrelated enveloped virus results in production of phenotypically mixed retroviral particles that carry spike proteins of both viruses (reviewed in reference 61). In fact, it has been demonstrated that a functional retroviral envelope can be entirely composed of spike proteins of foreign origin, i.e., particles defined as pseudotypes can be formed (6, 13, 15, 17, 32, 33, 53, 56). Furthermore, there are reports describing that certain cellular proteins can be assembled into the retroviral envelope (7, 29, 34), some even in high amounts (2, 59). This inclusion of heterologous proteins into virions has challenged the concept that core-spike interactions are necessary for incorporation of spike proteins into retroviral envelopes.

As a first step towards elucidating the mechanism by which retroviral spike proteins are included into virions, it is necessary to consider the relative incorporation efficiencies of homologous spike proteins versus heterologous membrane proteins. For example, in the majority of the reported cases of phenotypic mixing it has been impossible to say how efficiently the heterologous spike was incorporated, as its presence in the viral envelope was only demonstrated functionally, e.g., by expansion of the viral host range and/or by resistance of viral progeny to neutralizing antibodies directed against homologous spikes. It is possible that only few foreign spike proteins are sufficient to confer the above-mentioned properties in such assays. However, there have been three reports that claim that heterologous proteins can be incorporated into retroviral envelopes with efficiencies essentially similar to those of the respective homologous spike proteins when measured by biochemical assays (2, 13, 32).

In this study, incorporation of homologous and heterologous proteins into the envelope of Moloney murine leukemia virus (M-MuLV) has been analyzed by utilizing a Semliki Forest virus (SFV)-driven M-MuLV assembly system and quantitative biochemical assays. Contrary to the above-mentioned three reports (2, 13, 32), the results presented here clearly demonstrate that the homologous M-MuLV spike protein is preferentially incorporated into the M-MuLV envelope compared with the heterologous proteins tested. Efficient incorporation of heterologous proteins into the M-MuLV envelope was observed only when these proteins were expressed at very high densities at the plasma membrane.

MATERIALS AND METHODS

Plasmid constructs. (i) pSFV1-Pr65^{gag}. Plasmid pSFV1-Pr65^{gag} contains a DNA copy of the M-MuLV Pr65^{gag} gene under the SFV subgenomic promoter in pSFV1 (35). The Pr65^{gag} gene from pNCA (9) was inserted into pSFV1 as a 1,770-bp *Pst*I-*Dra*III fragment via subcloning steps in pGEM-1 and pGEM-7Zf(+) (Promega). As a result of the subcloning steps the Pr65^{gag} gene was flanked by *Bam*HI and *Sma*I sites at the 5′ and 3′ ends, respectively. Subsequently, the 5′ noncoding M-MuLV sequences preceding the Pr65^{gag} initiator methionine were deleted by replacing the 5′ 177-bp *Bam*HI-*Pst*I fragment of the Pr65^{gag} gene with a synthetic 135-bp *Bam*HI-*Pst*I fragment, which was created from the following two overlapping oligonucleotides: (i) 5′ ATTCTGATTGGATC

* Corresponding author. Mailing address: Department of Molecular Biology, Karolinska Institute, Novum, S-141 57 Huddinge, Sweden. Phone: 46-8-608 91 29. Fax: 46-8-774 55 38.

CAGCACCATGGGCCAGACTGTTACCACTCCCTTAA GTTTGACCTTAGGTCACTGGAAAGATGTCGAGCGG ATCGCTCACAACCAG 3′ and (ii) 5′ GGTTGGCCATTCT GCAGAGCAGAAGGTAACCCAACGTCTCTTCTTGAC ATCTACCGACTGGTTGTGAGCGATCCGCTCGACAT CTTTCCAGTGACCTAA 3′ (19). pSFV1-Pr65^{gag} serves as a template for in vitro production of recombinant SFV-Pr65^{gag} RNA.

(ii) pSFV-C/Pr65^{gag}. In pSFV-C/Pr65^{gag} the coding sequence of M-MuLV Pr65^{gag} is fused to the C gene of SFV. The fusion of the C gene to the second codon of the Pr65^{gag} gene was carried out by PCR (28, 58) with Vent$_R$ DNA polymerase (New England Biolabs) as recommended by the manufacturer. The terminal primers used for the amplification of the fused DNA were 5′ CAACGGAAAAACGCAGCAGC 3′ (the 5′-end primer) and 5′ CAAGGCTTCCCAGGTCACG 3′ (the 3′-end primer). The fusion primers used were 5′ GGGAGT GGTAACAGTCTGGCCCCACTCTTCGGACCCCTCGGG 3′ (C gene fragment primer) and 5′ CCCGAGGGGTCCG AAGAGTGGGGCCAGACTGTTACCACTCCC 3′ (Pr65^{gag} gene fragment primer). The pSFV-C/Pr65^{gag} was constructed by ligating the 562-bp *Csp*45I-*Pst*I C-Pr65^{gag} fusion fragment to the 10,679-bp *Spe*I-*Csp*45I fragment of pSFV-C (52) and the 2,492-bp *Pst*I-*Spe*I fragment of pSFV1-Pr65^{gag}. The 562-bp *Csp*45I-*Pst*I fragment of pSFV-C/Pr65^{gag} originating from the PCR was checked by sequencing. The RNA transcribed from pSFV-C/Pr65^{gag} was named SFV-C/Pr65^{gag}.

(iii) pSFV1-Pr80^{env}. Plasmid pSFV1-Pr80^{env} contains a DNA copy of the M-MuLV Pr80^{env} gene under the SFV subgenomic promoter in pSFV1 (35). The Pr80^{env} cDNA from pNCA (9) was inserted into the *Sma*I site of pSFV1 as a 2,080-bp *Xba*I-*Nhe*I fragment via subcloning steps in pGEM-7Zf(+) and M13mp18 (GIBCO-BRL). The internal *Spe*I sites in the Pr80^{env} coding sequence had been removed by site-directed mutagenesis, using 5′ GGCCATGCTGTCTCTCAC GAGTCCTGTGTGGTCCGCATA 3′ as the mutating oligonucleotide (50). The recombinant SFV genome transcribed from pSFV1-Pr80^{env} was named SFV-Pr80^{env}.

(iv) pSFV1-Pr65^{gag}+Pr80^{env}. Plasmid pSFV1-Pr65^{gag}+Pr80^{env} contains two promoters for subgenomic RNA transcription: a 3′ proximal promoter on the negative strand directs the synthesis of the mRNA for M-MuLV Pr65^{gag}, and the 3′ distal promoter directs the synthesis of the mRNA for M-MuLV Pr80^{env}. pSFV1-Pr65^{gag}+Pr80^{env} was made by replacing the 75-bp *Xba*I-*Bgl*II fragment of pSFV1-Pr80^{env} with the 2,493-bp *Xba*I-*Sma*I fragment from pSFV1-Pr65^{gag}. The *Bgl*II site was filled in with Klenow fragment prior to ligation. The RNA transcribed from pSFV1-Pr65^{gag}+Pr80^{env} was named SFV-Pr65^{gag}+Pr80^{env}.

(v) pSFV1-p62*E1. pSFV1-p62*E1 contains a DNA copy of the spike protein-encoding region of SFV 26S RNA under the SFV subgenomic promoter. pSFV-p62*E1 is otherwise similar to the previously described pSFV-spike (52), except that the gene region defining the endoprotease cleavage site of p62 is mutated on pSFV-p62*E1 (4). Construction of pSFV-p62*E1 is described elsewhere (3). The RNA transcribed from pSFV-p62*E1 was named SFV-p62*E1.

(vi) pSFV1-Pr65^{gag}+p62*E1. Plasmid pSFV1-Pr65^{gag}+p62*E1 is otherwise similar to pSFV1-Pr65^{gag}+Pr80^{env} with the exception that the 3′ distal promoter on the negative strand directs the synthesis of the mRNA for the SFV spike proteins. pSFV-Pr65^{gag}+p62*E1 was constructed by replacing the 75-bp *Xba*I-*Bgl*II fragment of pSFV1-p62*E1 with the 2,493-bp *Xba*I-*Sma*I fragment of pSFV1-Pr65^{gag}. The *Bgl*II site was filled in with Klenow fragment prior to ligation. The RNA transcribed from pSFV1-Pr65^{gag}+p62*E1 was named SFV-Pr65^{gag}+p62*E1.

(vii) pSFV-(E2Y399K). pSFV-(E2Y399K) is a derivative of pSP6-SFV4 (37) and contains a full-length cDNA clone of the SFV genome, but the codon specifying the tyrosine 399 in the cytoplasmic domain of E2 has been changed to a lysine codon. This mutation inhibits the budding of SFV (63) [this paper also contains a description of the construction of pSFV-(E2Y399K)]. The RNA transcribed from pSFV-(E2Y399K) is called SFV-(E2Y399K).

(viii) pSFV-C/TRΔ2. TRΔ2 is a mutant form of the human transferrin receptor, from which amino acids 6 to 53 in the cytoplasmic tail have been deleted. In pSFV-C/TRΔ2 the cDNA of the coding sequence of TRΔ2 is fused to the C gene of SFV. The precise fusion of C and TRΔ2 genes was carried out by PCR (28, 58). The terminal primers used for the amplification of the fused DNA were 5′ CAACGGAAAAA CGCAGCAGC 3′ (the 5′-end primer) and 5′ CTTTGCTG AGTTTAAATTCACG 3′ (the 3′-end primer). The fusion primers used were 5′ CATTGGCTTGATCCATCATCCACT CTTCGGACCCCTCGGG 3′ (C gene fragment primer) and 5′ CCCGAGGGGTCCGAAGAGTGGATGATGGATCAA GCCAATGTC 3′ (TRΔ2 gene fragment primer). pSFV-C/TRΔ2 was constructed by ligating the 756-bp *Csp*45I-*Nde*I fusion fragment to the 10,679-bp *Spe*I-*Csp*45I fragment of pSFV-C (52) and the 2,744-bp *Nde*I-*Spe*I fragment of pSFV1-TR (35). The 756-bp *Csp*45I-*Nde*I fragment of pSFV-C/TRΔ2 originating from the PCR was checked by sequencing. The RNA transcribed from pSFV-C/TRΔ2 was named SFV-C/TRΔ2.

RNA transcription, electroporation, and metabolic labelling of transfected cells. RNA transcripts were synthesized in vitro by SP6 RNA polymerase, with *Spe*I-digested plasmids as templates. Reaction conditions for in vitro RNA transcription have been described previously (37). In vitro-made RNA was transfected into BHK-21 cells (obtained from the American Type Culture Collection) by electroporation. Confluent cell monolayers were trypsinized, washed once with complete BHK medium (BHK-21 medium [GIBCO] supplemented with 5% fetal calf serum, 20 mM *N*-2-hydroxyethylpiperazine-*N*′-2-ethanesulfonic acid [HEPES; pH 7.3]) and once with ice-cold phosphate-buffered saline (PBS; without $MgCl_2$ and $CaCl_2$), and resuspended in 0.8 ml of PBS. The cell suspension was mixed with in vitro-made RNA (20 μl of the reaction mixture) and transferred to a 0.4-cm-diameter electroporation cuvette (Bio-Rad). In cotransfection experiments, equal amounts of both RNAs (20 μl) were used, except in the SFV-Pr65^{gag}+p62*E1 and SFV-Pr65^{gag}+Pr80^{env} cotransfections, in which twice as much SFV-Pr65^{gag}+p62*E1 RNA (30 versus 15 μl) was included into the transfection mixture in order to ensure a higher expression level for SFV spike proteins. Electroporation was carried out at room temperature by two consecutive pulses at 0.85 kV and 25 μF, with a Bio-Rad Gene Pulser apparatus (without the pulse controller unit). These conditions yielded virtually 100% transfection efficiencies. Electroporated cells were diluted into 18 ml of complete BHK medium, transferred onto tissue culture plates, and incubated at 37°C. At 8 h postelectroporation, culture media were replaced with methionine-free minimum essential medium (GIBCO) supplemented with 10 mM HEPES. After 30 min at 37°C, media were replaced with the same methionine-free medium containing 100 μCi of [^{35}S]methionine per ml, and cells were incubated at 37°C for 30 min. After the 30-min pulse, cells were washed once with BHK-21 medium containing 10 mM HEPES and a 10-fold excess of cold methionine and then incubated in the same medium for 15 min to 4 h (chase). Alternatively, cells

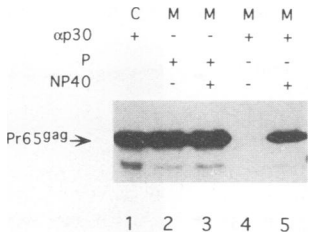

FIG. 1. Assembly of Pr65^{gag} into extracellular virus-like particles. SFV-Pr65^{gag}-transfected cells were metabolically labelled with [^{35}S]methionine for 4 h, and the amount of Pr65^{gag} in equal volumes of cell lysates (C; lane 1) and culture media (M; lanes 2 to 5) was analyzed. αp30, immunoprecipitation with the anti-p30 antiserum; P, particulate fractions of the culture media; NP40, solubilization of culture media with NP-40 (0.5% in lane 3 and 1% in lane 5).

were continuously labelled for 4 h with [^{35}S]methionine (100 μCi/ml). After the chase (or the 4-h pulse-labelling), culture media were collected and clarified by centrifugation in an Eppendorf centrifuge (5 min at 5,000 rpm at 4°C). Cell monolayers were washed with PBS and solubilized with 1% sodium dodecyl sulfate (SDS) or 1% Nonidet P-40 (NP-40) lysis buffers containing 10 mM iodoacetamide (42, 51). Nuclei were removed from cell lysates by centrifugation in an Eppendorf centrifuge (5 min at 5,000 rpm at 4°C).

Immunoprecipitation of proteins from cell lysates. M-MuLV Pr65^{gag} proteins were immunoprecipitated from SDS-solubilized cell lysates with a polyclonal rabbit anti-p30 antiserum (a generous gift from G. Schmidt, Institut für Molekulare Virologie, GSF, Munich, Germany) or with a polyclonal pig anti-MuLV antiserum (HC 185; Quality Biotech Inc.). M-MuLV Pr80^{env} and Pr15E proteins were immunoprecipitated from NP-40-solubilized cell lysates with the polyclonal anti-MuLV antiserum. SFV nucleocapsid protein C and spike proteins p62/E2 and E1 were immunoprecipitated from NP-40-solubilized cell lysates with monoclonal anti-C (36-1-9 [24]) and monoclonal anti-E1 (UM 8.139 [5]) antibodies, respectively. The monoclonal anti-E1 antibody also coprecipitates the p62/E2 subunit of the spike heterodimer. Human transferrin receptor mutant TRΔ2 was immunoprecipitated from NP-40-solubilized cell lysates with a monoclonal anti-TR antibody (the kind gift of T. Ebel). Immunocomplexes were brought down with protein A-Sepharose (Pharmacia; 1:1 [vol/vol] slurry in 10 mM Tris-HCl [pH 7.5]), using rabbit anti-mouse immunoglobulins (Dakopatts a/s, Glostrup, Denmark) as linking antibodies when necessary. Immunoprecipitates were solubilized in SDS sample buffer (200 mM Tris-HCl [pH 8.8], 20% glycerol, 5 mM EDTA, 0.02% bromphenol blue, 4% SDS, 50 mM dithiothreitol) and analyzed by SDS-polyacrylamide gel electrophoresis (PAGE) as previously described (51), except that gels were processed for autoradiography without methanol-acetic acid fixing. Radioactivity in protein bands was quantitated as previously described (54).

Analysis of extracellular virus particles. M-MuLV Gag particles were harvested from clarified culture media by pelleting them through a 20% sucrose cushion in a Beckman JA 18.1 rotor at 17,000 rpm for 2 h at 4°C. Pelleted particles were taken up into SDS sample buffer and analyzed by SDS-PAGE. The particulate structure of extracellular Gag particles was analyzed by SDS-PAGE following detergent solubilization of the culture media samples and subsequent pelletation of these through 20% sucrose cushions. The particulate structure was found to be resistant to 0.5% NP-40 (Fig. 1, lane 3) but was disrupted to a significant degree by treatment with 1% NP-40 (data not shown).

Isopycnic centrifugation. Transfected cells were metabolically labelled with [^{35}S]methionine (200 μCi/ml) for 5 to 6 h. At the end of the pulse, culture media were collected and clarified by centrifugation in an Eppendorf centrifuge (5 min at 5,000 rpm at 4°C). Clarified culture media (1 ml) were loaded onto 20 to 50% (wt/wt) sucrose gradients in TNE buffer (50 mM Tris-HCl [pH 7.4], 100 mM NaCl, 1 mM EDTA) and subjected to centrifugation in a Beckman SW 28.1 rotor for 20 h at 25,000 rpm and at 4°C. Gradients were fractionated from the bottom, and the radioactivity in each fraction was determined by liquid scintillation counting. Aliquots from peak fractions were diluted 1:2 into TNE buffer and subjected to centrifugation in a JA 18.1 rotor for 2 h at 17,000 rpm and at 4°C. The pellet fraction was solubilized in SDS sample buffer and analyzed by SDS-PAGE.

Analysis of transport of membrane proteins to the cell surface. (i) M-MuLV spike proteins. SFV-Pr80^{env}-transfected cells were pulse-labeled for 30 min and chased for various times, up to 4 h. Duplicate plates for each time point were used. M-MuLV envelope proteins were immunoprecipitated from cell lysates with a polyclonal anti-MuLV antiserum, and the transport of Pr80^{env} to the cell surface was assayed by monitoring the cleavage of Pr80^{env} to Pr15E by SDS-PAGE.

(ii) SFV spike proteins. Transport of SFV spike proteins to the cell surface was assayed by monitoring the conversion of E1-associated oligosaccharides to an endo-β-*N*-acetylglucosaminidase H (endo H)-resistant form. SFV-p62*E1- or SFV-(E2Y399K)-transfected cells were pulse-labeled for 30 min and chased for various times, up to 4 h. Duplicate plates for each time point were used. Spike protein complexes were immunoprecipitated from cell lysates with the monoclonal anti-E1 antibody, and immunoprecipitates were solubilized in endo H buffer (1% SDS, 50 mM sodium citrate [pH 6.0], with or without 50 mM dithiothreitol), incubated at 72°C (unreduced samples) or at 95°C for 4 min, and divided into two equal aliquots. One of the aliquots received 5 mU of endo H (Boehringer Mannheim), whereas endo H was omitted from the other. Samples were incubated at 37°C for 6 h, after which an equal volume of 2× SDS sample buffer was added, and samples were then analyzed by SDS-PAGE. Alternatively, the transport was assayed by monitoring the cleavage of p62 to E2 by SDS-PAGE.

(iii) TRΔ2. Transport of TRΔ2 to the cell surface was studied by a trypsin susceptibility assay. SFV-C/TRΔ2-transfected cells were pulse-labeled for 30 min and chased for either 15 min or 4 h. Duplicate plates for each time point were used. At the end of the chase, culture media were removed and cell monolayers were placed on ice and washed twice with ice-cold PBS+ (PBS with $MgCl_2$ and $CaCl_2$), and 0.5 mg of trypsin per ml in PBS+ (0.3 ml/3-cm-diameter plate) was added. Trypsin cleaves plasma membrane-associated TRΔ2 into a defined soluble fragment, which is released into the incubation medium. After 1 h of incubation on ice in the cold room, trypsin treatment was stopped by adding 60 μl of soybean trypsin inhibitor (25 mg/ml in PBS+). Cells were removed from plates by gentle pipetting, and the cell suspension was transferred to an Eppendorf tube. Plates were rinsed once with 0.5 ml of PBS+ to ensure quantitative recovery of cells, the wash was pooled with the cell suspension, and the sample was subjected to centrifugation in an Eppendorf centrifuge (1,500 rpm for 5 min at 4°C). The cell pellet fraction contained the intracellular pool of TRΔ2, and the supernatant fraction contained plasma membrane-associated TRΔ2. TRΔ2 from the solubilized cell

pellets and supernatant fractions was immunoprecipitated with monoclonal anti-TR antibodies and analyzed by SDS-PAGE.

RESULTS

Expression of M-MuLV Gag and Env precursors from recombinant SFV genomes. To assay in a rapid and simple way the incorporation of proteins into the M-MuLV envelope, we set up a heterologous, SFV-driven M-MuLV assembly system. The gene for the M-MuLV Gag precursor was engineered into the pSFV1 vector under the SFV subgenomic promoter (35), and the resulting plasmid was used as a template for in vitro transcription of the corresponding recombinant SFV genome, SFV-Pr65^{gag}. Figure 1 shows an analysis of SFV-Pr65^{gag}-transfected BHK-21 cells. At 8 h posttransfection, cells were metabolically labelled with [^{35}S]methionine for 4 h, and the amount of cell-associated and extracellular Pr65^{gag} was determined. The recombinant SFV genome directed the synthesis of Pr65^{gag} proteins which were recognized by a polyclonal anti-p30 antiserum (Fig. 1, lane 1). The lower minor band in lane 1 is a degradation product of Pr65^{gag}. Pr65^{gag} proteins were also detected in clarified culture media (lanes 2 to 5). This extracellular Pr65^{gag} was in a particulate form, since the proteins were quantitatively pelleted through a 20% sucrose cushion when subjected to centrifugation (lane 2). Prior detergent solubilization of the culture medium with 0.5% NP-40 did not alter this fractionation profile, suggesting that Pr65^{gag} was assembled into structures similar to those of the immature retrovirus core (lane 3) (26). Extracellular Pr65^{gag} was recognized by anti-p30 antiserum only after detergent solubilization of the culture medium (lanes 4 and 5). This suggested that Pr65^{gag} resided in membrane-enclosed particles. To obtain further evidence for this, the Pr65^{gag} content of culture media was analyzed by isopycnic centrifugation on 20 to 50% sucrose gradients. Pr65^{gag} was found in particles that had a buoyant density of 1.14 to 1.16 g/ml (data not shown), a value similar to that reported for the wild-type M-MuLV particles (27). Taken together, these results indicated that Pr65^{gag} expressed from the recombinant SFV genome was efficiently assembled into extracellular virus-like particles.

M-MuLV spike proteins are synthesized as a 80-kDa precursor form, which upon transport to the cell surface is cleaved into a surface part gp70 and a transmembrane part Pr15E by a cellular protease (41, 57). Since this cleavage event occurs late during transport, i.e., most probably in the *trans* Golgi compartment or later (25), quantity of Pr80^{env} precursors which have been cleaved can be taken as a measure of the amount of this protein transported to the cell surface. Phenotypic analysis of M-MuLV spike proteins expressed from SFV-Pr80^{env} RNA is shown in Fig. 2. At 8 h posttransfection cells were pulse-labelled for 30 min, and cell lysates were prepared after various chase periods (15 min to 4 h). As shown in Fig. 2, lane 1, the SFV-Pr80^{env} RNA directed the synthesis of Pr80^{env} which was recognized by a polyclonal anti-MuLV antiserum and which comigrated on SDS-PAGE with Pr80^{env} synthesized in wild-type M-MuLV-infected cells (data not shown). With an increasing chase time, the Pr80^{env} precursor underwent processing to a faster-migrating form (Fig. 2, lanes 2 to 4). This represents the transmembrane part of the processed M-MuLV spike, Pr15E. The surface part of the processed spike, gp70, was not detected in appreciable amounts in either cell lysates or culture media, thus suggesting that the majority of gp70 was shed from Pr15E and degraded. Maximum level of Pr15E was reached after a 2-h chase, and there was no significant decrease in the amount of cell-associated Pr15E between the 2- and 4-h chase time points. Quantitation of two separate experiments

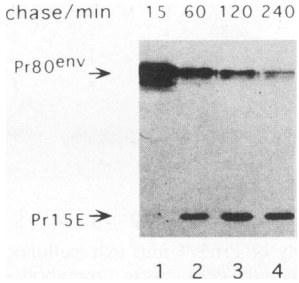

FIG. 2. Transport of M-MuLV spike proteins to the cell surface. SFV-Pr80^{env}-transfected cells were pulse-labelled for 30 min and chased for the indicated times. M-MuLV spike proteins were immunoprecipitated from cell lysates with the polyclonal anti-MuLV antiserum, and processing of Pr80^{env} to Pr15E was used as an indicator for transport of the spike proteins to the cell surface.

indicated that about 33% of synthesized Pr80^{env} was converted to Pr15E during the 4-h chase. Pr80^{env} that was not transported out of the endoplasmic reticulum was rapidly degraded.

To express the M-MuLV spike proteins together with Pr65^{gag}, a recombinant SFV-Pr65^{gag}+Pr80^{env} genome containing two promoters for subgenomic RNA transcription was constructed, and the genes for Pr65^{gag} and Pr80^{env} were placed separately under the control of these two promoters. Relative expression levels of Pr65^{gag} and Pr80^{env} in SFV-Pr65^{gag}+Pr80^{env}-transfected cells were analyzed from cell lysates that had been prepared after a 30-min pulse and a 15-min chase (see Fig. 5a, lane 1). After taking the relative numbers of methionine into consideration (three in Pr65^{gag} and eight in Pr80^{env}), quantitation of Pr65^{gag} and Pr80^{env} bands indicated that these proteins were expressed at similar levels. In order to assay incorporation of M-MuLV spike proteins into extracellular particles, SFV-Pr65^{gag}+Pr80^{env}-transfected cells were pulse-labelled for 4 h, and cell lysates and media samples were analyzed. Pr65^{gag}, Pr80^{env}, and Pr15E proteins were immunoprecipitated from cell lysates by the polyclonal anti-MuLV antiserum, and are shown in Fig. 3a, lane 1 (the heavy Pr80^{env} band partially hides the underlying Pr65^{gag} band). Particles that had been released into the culture media during the 4-h pulse were purified by pelletation through a sucrose cushion, and the protein composition of these particles is shown in Fig. 3a, lane 2. In addition to Pr65^{gag}, these particles also contained high amounts of Pr15E. The minor band above the Pr65^{gag} band in lane 2 is a form of Pr65^{gag} which is synthesized as a result of the suppression of the Pr65^{gag} stop codon (18) and represents an artefact of the construct. Extracellular Pr15E was most likely assembled into the envelope of the Gag particles, since no Pr15E was detected in culture media of control cells that were expressing only M-MuLV spike proteins (data not shown). To verify the physical association of Pr65^{gag} and Pr15E, material in the culture media of SFV-Pr65^{gag}+Pr80^{env}-transfected cells was analyzed by equilibrium density sedimentation. Pr15E was found to cofractionate with Pr65^{gag}, and the majority of both proteins were in particles that banded at a density of 1.14 to 1.16 g/ml (Fig. 3b). The radioactivity in Pr65^{gag} and Pr15E bands was quantitated, and after taking the relative numbers of methionine into consideration (three in Pr65^{gag} and five in Pr15E), the average ratio of Pr65^{gag} to Pr15E was estimated to be 5:1. This ratio is similar to the ratio of p30 to spike proteins in functional M-MuLV particles (32). Taken together, these results indicated that homologous M-MuLV spike proteins were efficiently assembled into extracellular Gag particles.

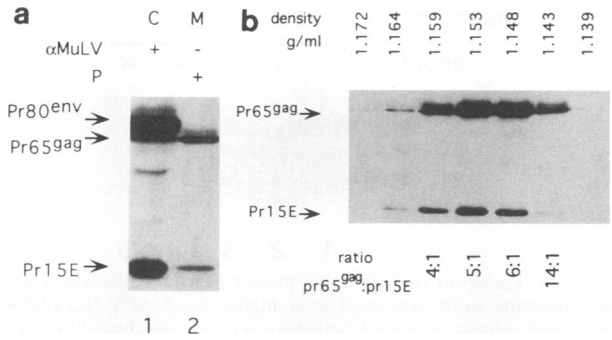

FIG. 3. Assembly of the homologous M-MuLV spike proteins into extracellular particles. (a) SFV-Pr65^{gag}+Pr80^{env}-transfected cells were pulse-labelled for 4 h, and M-MuLV proteins in cell lysates (C; lane 1) and clarified culture media (M; lane 2) were analyzed. αMuLV, immunoprecipitation with the anti-MuLV antiserum; P, particulate fraction of the culture media. (b) Particles released from the SFV-Pr65^{gag}+Pr80^{env}-transfected cells were analyzed by isopycnic centrifugation on a 20 to 50% sucrose gradient. The gradient was fractionated from the bottom, and radioactivity in the fractions was measured by liquid scintillation counting. Aliquots of peak fractions were diluted with TNE buffer, and M-MuLV particles in these fractions were isolated by pelletation. The pellet fraction was solubilized directly into SDS sample buffer and analyzed by SDS-PAGE.

Homologous spike proteins are more efficiently incorporated into extracellular M-MuLV particles than the heterologous SFV spike proteins. The spike protein complex of SFV was chosen as a probe to test the incorporation of a heterologous spike protein into extracellular Gag particles. The SFV spike complex is composed of two integral membrane proteins, p62 and E1, which form a heterodimeric complex in the endoplasmic reticulum (36, 54, 64). The p62 subunit is cleaved by a host protease in its external domain late during transport of the spike heterodimer to the cell surface (11). This cleavage event generates the E2 form found in mature virions. However, in the experiments described below a mutant form of p62 (the p62*) that does not undergo this processing event because of a mutation at the cleavage site was used (4). This mutant form was chosen instead of the wild-type protein, because control experiments have established that this unprocessed p62*-E1 spike complex is more stably expressed at the cell surface than the mature E2-E1 complex (3).

In order to reliably evaluate the efficiency of incorporation of the SFV spike relative to that of the M-MuLV spike, it was first important to assess expression of SFV spike proteins at the cell surface and compare this to that of the M-MuLV spike proteins studied above. SFV spike proteins were expressed from SFV-p62*E1 RNA, and at 8 h posttransfection, cells were pulse-labelled for 30 min and chased for various times, up to 4 h. SFV spike proteins were immunoprecipitated from cell lysates by a monoclonal E1 antibody, and transport of the spike complex to the cell surface was monitored by following the conversion of E1-associated carbohydrate chains to an endo H-resistant form. As shown in Fig. 4, some E1 proteins had acquired endo H-resistant sugars after 15 min of chase, and the amount of endo H-resistant E1 increased up to the 4-h chase point. Quantitation of two separate experiments indicated that about 29% of synthesized E1 was converted to the endo H-resistant form during the 4-h chase. Although endo H-resistance only indicates transport to the medial Golgi (16), separate control experiments have established that the p62*-E1 complex is transported all the way to the plasma membrane because it is efficiently rescued into virus particles

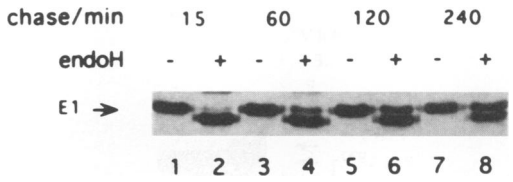

FIG. 4. Transport of the SFV p62*-E1 complex to the cell surface. SFV-p62*E1-transfected cells were pulse-labelled for 30 min and chased for the times indicated. Conversion of E1-associated oligosaccharides to the endo H-resistant form was monitored and used as an indicator for transport of the spike complex to the cell surface.

when coexpressed with SFV nucleocapsids (3). Therefore, within the limitations of the methods used to estimate transport, it was concluded that the p62*-E1 complex was transported to the cell surface as efficiently as the M-MuLV spike proteins analyzed above (33% of synthesized M-MuLV spike proteins had reached the cell surface after a 4-h chase).

For coexpression of Pr65^{gag} and SFV spike proteins, we constructed a recombinant SFV-Pr65^{gag}+p62*E1 genome, in which the Pr65^{gag} and the SFV spike protein genes were placed under separate subgenomic promoters. Since our control experiments had indicated that the expression level of Pr65^{gag} relative to that of the membrane protein can greatly influence the apparent incorporation efficiency of the membrane protein, inclusion of M-MuLV and SFV spike proteins into extracellular particles was compared by cotransfecting SFV-Pr65^{gag}+Pr80^{env} and SFV-Pr65^{gag}+p62*E1 RNAs into BHK-21 cells. Twice as much SFV-Pr65^{gag}+p62*E1 RNA as SFV-Pr65^{gag}+Pr80^{env} RNA was included into the transfection mixture to ensure a higher expression level of the SFV spike proteins. Relative expression levels of Pr80^{env} and p62*-E1 were examined from cell lysates that had been prepared after a 30-min pulse and a 15-min chase. M-MuLV proteins were immunoprecipitated from cell lysates by the polyclonal anti-MuLV antiserum, and SFV spike proteins by the monoclonal anti-E1 antibodies; the latter antibodies also coprecipitate the p62 subunit of the spike heterodimer. As shown in Fig. 5a, lanes 2 (anti-MuLV immunoprecipitation) and 3 (anti-E1 immunoprecipitation), SFV spike proteins were expressed at a higher level than M-MuLV spikes: quantitation of Pr80^{env} and E1 bands indicated that E1 was synthesized at about a four-fold-higher level than Pr80^{env}. The protein comigrating with Pr65^{gag} in lane 3 is p62*, and the apparently smaller amount of

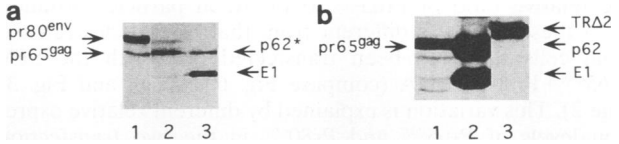

FIG. 5. Comparison of protein expression in transfected cells. Cells were pulse-labelled for 30 min, chased for 15 min, and solubilized. Equal volumes of cell lysates were subjected to immunoprecipitation by anti-MuLV antiserum, anti-E1 antibodies, or anti-TR antibodies. (a) Lane 1, protein expression in SFV-Pr65^{gag}+Pr80^{env}-transfected cells; lane 2 (anti-MuLV immunoprecipitation) and lane 3 (anti-E1 immunoprecipitation), protein expression in SFV-Pr65^{gag}+Pr80^{env}- and SFV-Pr65^{gag}+p62*E1-cotransfected cells. (b) Lanes 1 and 2, expression levels of Pr65^{gag} and SFV spike proteins respectively, in SFV-C/Pr65^{gag}- and SFV-(E2Y399K)-cotransfected cells; lane 3, TRΔ2 that was immunoprecipitated from SFV-C/Pr65^{gag}- and SFV-C/TRΔ2-cotransfected cell lysates. The lanes originate from different gels, but the exposure times on film were similar.

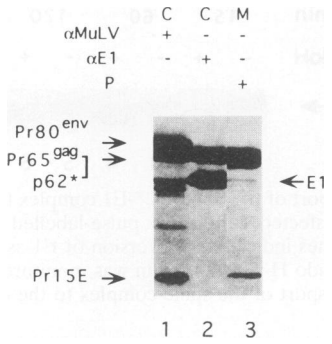

FIG. 6. Comparison of incorporation of M-MuLV and SFV spike proteins into extracellular particles. SFV-Pr65^{gag}+Pr80^{env}- and SFV-Pr65^{gag}+p62*E1-cotransfected cells were pulse-labelled for 4 h, and cell-associated proteins (C; lanes 1 and 2) and extracellular particles were analyzed. αMuLV, immunoprecipitation by the anti-MuLV antiserum; αE1, immunoprecipitation by the monoclonal anti-SFV E1 antibodies; P, particulate fraction of the culture media (M). Note that the film is overexposed to bring out the faint E1 band in the medium. The bands between Pr65^{gag} and Pr15E in lane 1 are degradation products of Pr65^{gag} and Pr80^{env}.

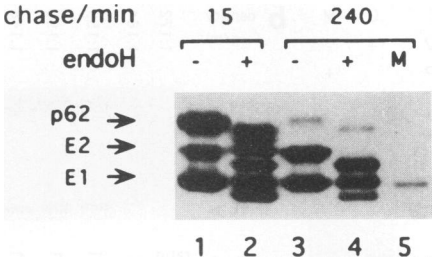

FIG. 7. Transport of SFV spike proteins to the cell surface when these proteins were expressed at a higher level. SFV-(E2Y399K)-transfected cells were pulse-labelled for 30 min and chased for either 15 min or 4 h. Aliquots of samples at each time point were analyzed by endo H digestion. The conversion of E1-associated oligosaccharides to the endo H-resistant form and the processing of p62 to E2 indicate transport of the spike complex to the cell surface. Lane 5, analysis of the solubilized 4-h chase medium by immunoprecipitation with anti-E1 antibodies.

the latter protein in comparison to E1 is due to inefficient coprecipitation of p62* by the monoclonal anti-E1 antibody. Since M-MuLV and SFV spike proteins were transported to the cell surface with similar efficiencies (see above), the higher synthesis level of SFV spike proteins should ensure a higher expression of SFV spikes at the cell surface. To examine incorporation of Pr15E and p62*-E1 proteins into extracellular particles under these conditions, SFV-Pr65^{gag}+Pr80^{env}- and SFV-Pr65^{gag}+p62*E1-cotransfected cells were pulse-labelled for 4 h, and cell lysates and culture media were analyzed. Cell-associated Pr80^{env}, Pr65^{gag}, and Pr15E are shown in Fig. 6, lane 1, and intracellular p62* and E1 are shown in lane 2. Extracellular particles were isolated by pelletation through a sucrose cushion, and the protein composition of these particles is shown in lane 3. Pr15E was readily detectable in these particles, but in contrast, only trace amounts of E1 could be detected (the p62* band was not visible, because it was hidden by the Pr65^{gag} band). Similar results were obtained if the wild-type SFV E2-E1-spike complex was used instead of the cleavage-deficient p62*-E1 complex (data not shown). Therefore, it can be concluded that the homologous M-MuLV spike is preferentially incorporated into the M-MuLV envelope in comparison to the heterologous SFV spike complex. Note, that the relative ratio of Pr65^{gag} to Pr15E in particles produced from these cells was different from that in particles released from cells that had been transfected only with the SFV-Pr65^{gag}+Pr80^{env} RNA (compare Fig. 6, lane 3, and Fig. 3a, lane 2). This variation is explained by different relative expression levels of Pr65^{gag} and Pr80^{env} in the two transfections (compare lanes 1 and 2 in Fig. 5a) and demonstrates the influence that the expression level of the core protein relative to that of the membrane protein has on the apparent incorporation efficiency of the membrane protein.

We also analyzed the incorporation of a mutant form of the human transferrin receptor, TRΔ2. The TRΔ2 mutant is a homodimeric plasma membrane protein, but it differs from its wild-type counterpart by having an extensive deletion at the cytoplasmic domain. This deletion has removed the internalization signal of the transferrin receptor and has thus rendered the TRΔ2 mutant defective in endocytosis (10, 31). When TRΔ2 was coexpressed with Pr65^{gag}, no TRΔ2 was detected in extracellular particles, although control experiments indicated that TRΔ2 was expressed at a level at the plasma membrane similar to those of the M-MuLV spike proteins (data not shown).

Increased expression of SFV spike proteins at the cell surface results in efficient incorporation of these proteins into extracellular particles. In the experiments described above, M-MuLV and SFV spike proteins were expressed at relatively low densities at the plasma membrane, i.e., each was at a density comparable to that of M-MuLV spike proteins in wild-type M-MuLV infection. It was of interest to see whether the SFV spike complex would be more efficiently incorporated into extracellular particles when the spike was present at a higher density at the plasma membrane. Analysis of the protein expression in cells transfected with different SFV expression vectors have established that the SFV-driven expression system yields a considerably higher level of expression for a given protein if the coding unit of the protein is fused to the C gene of SFV (48). In order to achieve a high expression of SFV spike proteins, SFV-(E2Y399K) RNA, which contains the complete structural coding region of SFV (C-p62-E1), was used in the experiments described below. SFV-(E2Y399K) is otherwise similar to the wild-type genome of SFV, except that SFV-(E2Y399K) contains a point mutation which results in a tyrosine to lysine substitution at position 8 in the cytoplasmic tail of p62/E2. This mutation does not affect the transport of spike heterodimers to the cell surface, but it abolishes the interactions of spike proteins with the viral nucleocapsid and thus inhibits the budding of SFV (63) (Fig. 7, lane 5). Therefore, cells infected with this mutant RNA synthesize high amounts of viral nucleocapsids and spike proteins, which accumulate in cytoplasm and plasma membrane, respectively. Comparison of spike protein expression levels in either SFV-(E2Y399K)-transfected cells or SFV-Pr65^{gag}+p62*E1-transfected cells indicated that SFV-(E2Y399K) RNA yielded greater than a 10-fold-higher expression (compare Fig. 5a, lane 3, and Fig. 5b, lane 2). The control experiment shown in Fig. 7 demonstrated that most of the newly synthesized spike heterodimers in SFV-(E2Y399K)-transfected cells were indeed efficiently transported to the cell surface. Transfected cells were pulse-labelled for 30 min and chased for either 15 min or 4 h. Transport of spike heterodimers to the cell surface was followed by monitoring the conversion of E1-associated oligosaccharides to the endo H-resistant form, as well as by assaying the cleavage of p62 to E2 (11). A substantial fraction of E1

proteins had acquired endo H-resistant sugars after the 15-min chase, and after 4 h the majority of the cell-associated E1 was of the endo H-resistant form. Quantitation of three separate experiments indicated that the endo H-resistant E1 at the 4-h chase point comprised about 51% of total E1 synthesized during the 30-min pulse. The cleavage of p62 to E2 followed a similar kinetics: E2 present at the 4-h chase point was found to constitute about 48% of the total p62 synthesized (p62 + E2 at the 15-min chase point). Therefore, it can be concluded that the higher synthesis level of SFV spike proteins in SFV-(E2Y399K)-transfected cells resulted in a comparable increase in the expression of these proteins at the cell surface. Solubilized culture media from the 4-h chase point were also analyzed for the presence of spike proteins by immunoprecipitation with anti-E1. As shown in Fig. 7, lane 5, only a small amount of a protein fragment migrating slightly faster than intracellular E1 was detected in these culture media. This corresponds to a soluble form of E1, which is released into culture medium probably as a result of a host-mediated cleavage of some proportion of cell-surface spike complexes (62).

In order to increase the overall production of extracellular Gag particles, the expression level of $Pr65^{gag}$ was elevated by fusing the coding sequence of $Pr65^{gag}$ to the C gene of SFV. This created the recombinant SFV genome SFV-C/$Pr65^{gag}$, which expresses $Pr65^{gag}$ as a C-$Pr65^{gag}$ fusion protein. The fusion protein is cotranslationally processed into C and $Pr65^{gag}$ proteins by the autoproteolytic activity of the C protein (Fig. 8a) (1, 8, 20, 39). Comparison of $Pr65^{gag}$ expression levels in Fig. 5a, lane 1 (SFV-$Pr65^{gag}$+$Pr80^{env}$-transfected cells) and Fig. 5b, lane 1 (SFV-C/$Pr65^{gag}$- and SFV-(E2Y399K)-cotransfected cells) indicated that the use of the SFV-C/$Pr65^{gag}$ RNA increased the $Pr65^{gag}$ expression by about 10-fold. Analyses of $Pr65^{gag}$ proteins expressed from the SFV-C/$Pr65^{gag}$ RNA have shown that the proteins are correctly modified by myristylation at their amino termini, and the proteins become efficiently assembled into extracellular virus-like particles (data not shown).

Incorporation of SFV spike proteins into extracellular particles under high expression of these proteins at the cell surface was assayed following cotransfection of BHK-21 cells with SFV-C/$Pr65^{gag}$ and SFV-(E2Y399K) RNAs. At 8 h after transfection, cells were pulse-labelled for 30 min and chased for 4 h, and cell-associated and extracellular proteins were analyzed. SFV nucleocapsid protein C and SFV spike proteins were immunoprecipitated from cell lysates by monoclonal anti-C and monoclonal anti-E1 antibodies, respectively, and are shown in Fig. 8a, lanes 1 (C) and 3 (spike proteins). Because of the long chase time (4 h), the majority of the intracellular spike complexes were in the mature E2-E1 form. Cell-associated $Pr65^{gag}$ proteins, immunoprecipitated by the polyclonal anti-MuLV antiserum, are shown in lane 2. Particles which had been released into the culture media during the 4-h chase were purified by pelletation through a sucrose cushion, and the protein composition of these particles is shown in lane 4. By comparing the ratio of $Pr65^{gag}$ to E2 and E1, it is evident that the particulate fraction now contained high amounts of the SFV spike proteins. To verify that these proteins were incorporated into the envelope of Gag particles, the material in culture media was subjected to equilibrium density sedimentation. Analyses of gradient fractions demonstrated that E2 and E1 cofractionated with $Pr65^{gag}$, and the majority of the proteins were found in particles that banded at a density of 1.14 to 1.18 g/ml (Fig. 8b; E2 and E1 proteins comigrated as electrophoresis was under reducing conditions). After taking the relative numbers of methionine into consideration (3 in

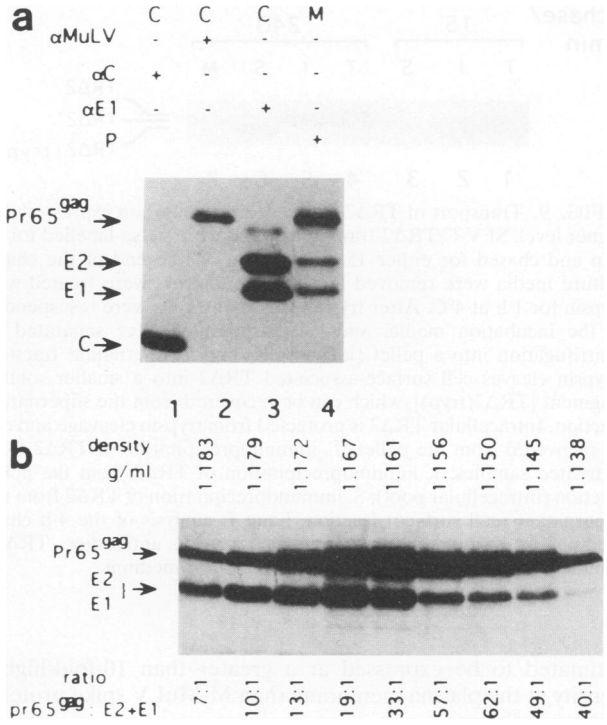

FIG. 8. Incorporation of SFV spike proteins into extracellular particles in SFV-C/$Pr65^{gag}$- and SFV-(E2Y399K)-cotransfected cells. (a) Transfected cells were pulse-labelled for 30 min and chased for 4 h. Lanes 1 to 3, analyses of cell lysates (C); lane 4, analysis of the corresponding culture medium (M). αMuLV, αC, and αE1, immunoprecipitation by anti-MuLV antiserum, by anti-SFV C antibodies, and by anti-SFV E1 antibodies, respectively. P, particulate fraction of the culture medium. (b) Analysis of extracellular particles by isopycnic centrifugation on a 20 to 50% sucrose gradient. This experiment was done as described in the legend to Fig. 3b, and peak fractions of the gradient are shown. Note that E2 and E1 comigrated as the electrophoresis was under reducing conditions.

$Pr65^{gag}$ and 17 in E2-E1), quantitations indicated that the average relative ratio of $Pr65^{gag}$ to E2-E1 was 26:1. However, the particles clearly differed in their spike contents: the heavier particles contained high amounts of E2-E1, whereas the spike density was significantly lower in the lighter particles. Taken together, the results described in this section demonstrate that the SFV spike complex is efficiently assembled into extracellular particles, providing that the spike is expressed at a high density at the plasma membrane. This high level of incorporation was independent of the overall budding efficiency, since similar results were obtained if SFV-$Pr65^{gag}$ RNA (i.e., that with the low level of expression) was used for the expression of $Pr65^{gag}$ instead of the SFV-C/$Pr65^{gag}$ RNA described here (data not shown).

Unfortunately, it was not possible to directly compare incorporation of SFV spike proteins with that of M-MuLV spikes under high expression of these proteins at the cell surface, since when $Pr80^{env}$ was expressed at a high level (i.e., as a C fusion protein), the bulk of spike proteins was not transported out of the endoplasmic reticulum (data not shown). However, particles produced from cells cotransfected with SFV-$Pr65^{gag}$+$Pr80^{env}$ RNA, which expressed at the low level, and SFV-(E2Y399K) RNA, which expressed at the high level, contained roughly equal amounts of Pr15E and SFV spikes. This was despite the fact that SFV spike proteins were

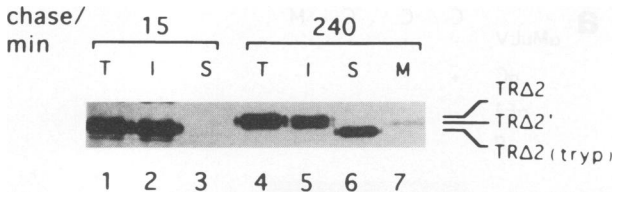

FIG. 9. Transport of TRΔ2 to the cell surface when expressed at a higher level. SFV-C/TRΔ2-transfected cells were pulse-labelled for 30 min and chased for either 15 min or 4 h. At the end of the chase, culture media were removed and cell monolayers were treated with trypsin for 1 h at 4°C. After trypsin treatment, cells were resuspended in the incubation media, and cell suspensions were separated by centrifugation into a pellet (intact cells) and a supernatant fraction. Trypsin cleaves cell surface-associated TRΔ2 into a smaller soluble fragment [TRΔ2(tryp)], which can be recovered from the supernatant fraction. Intracellular TRΔ2 is protected from trypsin cleavage and can be recovered from the pellet. T, immunoprecipitation of TRΔ2 from untreated samples; I, immunoprecipitation of TRΔ2 from the pellet fraction (intracellular pool); S, immunoprecipitation of TRΔ2 from the supernatant (cell surface) fraction. Lane 7, analysis of the 4-h chase medium by immunoprecipitation with anti-TR antibodies. TRΔ2', soluble TRΔ2 form recovered from the culture medium.

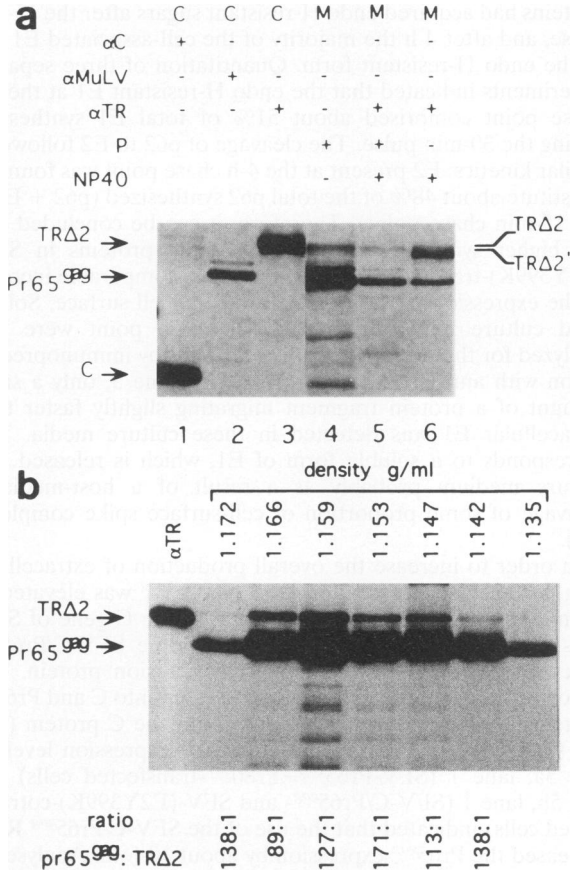

FIG. 10. Incorporation of TRΔ2 into extracellular particles in SFV-C/Pr65^{gag}- and SFV-C/TRΔ2-cotransfected cells. (a) Transfected cells were pulse-labelled for 30 min and chased for 4 h. Lanes 1 to 3, analyses of cell lysates (C); lanes 4 to 6, analyses of the corresponding culture media (M). αMuLV, αC, and αTR, immunoprecipitation with anti-MuLV antiserum, with anti-SFV C antibodies, and with anti-TR antibodies, respectively; P, particulate fraction of the culture media; NP40, solubilization with 1% NP-40. TRΔ2' indicates the soluble form of TRΔ2 released into the culture medium. (b) Analysis of extracellular particles by isopycnic centrifugation on a 20 to 50% sucrose gradient. The experiment was done as described in the legend to Fig. 3b, and peak fractions of the gradient are shown. The leftmost first lane (αTR) shows marker TRΔ2 proteins immunoprecipitated from SFV-C/TRΔ2-transfected cell lysates.

estimated to be expressed at a greater than 10-fold-higher density at the plasma membrane than M-MuLV spike proteins (data not shown).

A cellular plasma membrane protein is also incorporated into M-MuLV particles when the protein is expressed at a high level at the cell surface. Whether or not the cellular TRΔ2 protein would be incorporated into extracellular particles when both Pr65^{gag} and TRΔ2 were expressed at a high level was next examined. To achieve a high expression level of TRΔ2, recombinant SFV genome SFV-C/TRΔ2 in which the coding sequence of the TRΔ2 protein was fused to the C gene of SFV was constructed. The C-TRΔ2 fusion protein encoded by this RNA was correctly processed to C and TRΔ2 by the autoproteolytic activity of the C protein (see, e.g., Fig. 10a). Comparison of protein expression from SFV-C/TRΔ2 and SFV-(E2Y399K) RNAs indicated that TRΔ2 was synthesized at a two- to threefold-lower level than SFV spike proteins (Fig. 5b, lanes 2 and 3). In order to determine the proportion of TRΔ2 that was transported to the cell surface, SFV-C/TRΔ2-transfected cells were pulse-labelled for 30 min and chased for either 15 min or 4 h, and at the end of the chase cell monolayers were treated with trypsin at 4°C for 1 h. After trypsin treatment, cells were resuspended in the incubation medium, and the cell suspension was separated by centrifugation into a pellet (intact cells) and a supernatant fraction. Trypsin cleaves cell surface-associated TRΔ2 into a smaller soluble fragment, which can be recovered from the supernatant fraction. In contrast, intracellular TRΔ2 is protected from trypsin cleavage and remains cell associated. TRΔ2 from pellet and supernatant fractions was immunoprecipitated by a monoclonal anti-human transferrin receptor antibody (anti-TR). As shown in Fig. 9, all TRΔ2 was intracellular after a 15-min chase, whereas the majority of cell-associated TRΔ2 had reached the cell surface after 4 h. As described before (40), the TRΔ2 that had been transported to the cell surface was converted to a more slowly migrating form. Quantitations indicated that plasma membrane-associated TRΔ2 at the 4-h chase point comprised about 29% of total TRΔ2 synthesized during the 30-min pulse. Intracellular TRΔ2 at the 4-h chase point was resolved into two closely migrating bands, and the faster-migrating form of these (TRΔ2') could also be detected in the culture media of the 4-h chase point (Fig. 9, lane 7). This suggested that the faster-migrating variant was a soluble derivative of TRΔ2, but the precise origin of this fragment was not further investigated.

To test whether TRΔ2 could be incorporated into extracellular M-MuLV particles, SFV-C/Pr65^{gag} and SFV-C/TRΔ2 RNAs were cotransfected into BHK-21 cells and analyzed as described for the SFV-C/Pr65^{gag} and SFV-(E2Y399K) cotransfections. Cell-associated SFV C, M-MuLV Pr65^{gag}, and TRΔ2 are shown in Fig. 10a, lanes 1, 2, and 3, respectively. Lane 4 shows the protein composition of particles that had been released into culture media during the 4-h chase period. A protein of size similar to that of intracellular TRΔ2 was detected in this particulate fraction. The efficient immunoprecipitation of this protein from the solubilized particulate fraction by anti-TR indicated that this protein indeed was TRΔ2 (Fig. 10a, lane 5). Some Pr65^{gag} was also precipitated,

but this most likely represented nonspecific reactivity of the antibody with some $Pr65^{gag}$ residing on intact core structures. TRΔ2 in the particulate fraction was not of the soluble TRΔ2′ form: by comparing lanes 5 and 6 in Fig. 10a, it is evident that TRΔ2 in the particulate fraction migrated more slowly than the soluble TRΔ2′ fragment immunoprecipitated from solubilized, unfractionated culture media. This strongly suggested that TRΔ2 was incorporated into the envelope of Gag particles. To gain further evidence for this, material in the culture media was subjected to isopycnic centrifugation. As shown in Fig. 10b, TRΔ2 could be detected in fractions which contained enveloped Gag particles. After taking the relative numbers of methionine into consideration (3 in $Pr65^{gag}$ and 12 in TRΔ2), quantitations indicated that the average relative ratio of $Pr65^{gag}$ to TRΔ2 was 125:1. Thus, it can be concluded that a cellular protein is also incorporated into the M-MuLV envelope in biochemically detectable amounts, if the protein is expressed at a high level at the plasma membrane. The relative ratio of $Pr65^{gag}$ to TRΔ2 in the particles would suggest that TRΔ2 was less efficiently incorporated than SFV spike proteins analyzed in the previous section (the average relative ratio of $Pr65^{gag}$ to E2-E1 was 26:1). However, TRΔ2 was expressed at a two- to threefold-lower level in the experiments than SFV spike proteins, and TRΔ2 was also less efficiently transported to the cell surface. Therefore, the differences in the two ratios can be at least partly explained by a lower density of TRΔ2 at the cell surface.

DISCUSSION

In this study we have determined the efficiencies with which homologous and heterologous membrane proteins are incorporated into M-MuLV particles by utilizing a SFV-driven M-MuLV assembly system and quantitative biochemical assays. The spike complex of the unrelated virus SFV and the cytoplasmically truncated TRΔ2 mutant of the human transferrin receptor were used as representatives of heterologous proteins. During the course of this study it became evident that two factors in the experimental conditions can greatly influence the apparent incorporation efficiency of a protein. These factors are (i) the expression level of the core protein relative to that of the membrane protein tested and (ii) the density of the membrane protein at the cell surface. The importance of the former factor is evidenced by the different amounts of Pr15E in particles produced from SFV-$Pr65^{gag}$+$Pr80^{env}$-transfected cells and in particles produced from SFV-$Pr65^{gag}$+$Pr80^{env}$- and SFV-$Pr65^{gag}$+p62*E1-cotransfected cells. The differential incorporation of SFV spike proteins under low and high expression at the cell surface demonstrates the importance of the latter factor. When experimental conditions were standardized with respect to these two factors, the results obtained clearly demonstrate that the efficiencies of incorporation of homologous and heterologous proteins differed markedly. When $Pr65^{gag}$ was expressed together with M-MuLV spike proteins at a low expression level, the homologous spikes were efficiently assembled into extracellular particles: the average relative ratio of $Pr65^{gag}$ to Pr15E in purified particles was 5:1. In contrast, when the SFV spike complex or TRΔ2 was coexpressed with $Pr65^{gag}$ at similar levels, only trace amounts of SFV spike proteins and no TRΔ2 were detected in extracellular particles. The density of SFV spike proteins and TRΔ2 at the cell surface had to be increased by about 10-fold before these heterologous proteins became relatively efficiently incorporated into extracellular particles. Therefore, our major conclusion is that the homologous spike protein was preferentially incorporated into M-MuLV particles in comparison to the heterologous proteins tested.

The generality of this conclusion is at present unclear. As mentioned in the introduction, there are three reports in the literature which would indicate that heterologous proteins can be as efficiently incorporated into retroviral envelopes as the respective homologous spike proteins. Landau and Littman (32) reported that the spike protein of Rous sarcoma virus (RSV) was incorporated with an essentially similar efficiency into M-MuLV particles as the homologous M-MuLV spike: extracellular particles contained only twice as much M-MuLV spike proteins as RSV spikes. However, it is unclear whether experimental conditions had been standardized with respect to the densities of the two spike proteins at the cell surface or whether the expression levels of the membrane proteins relative to that of the core protein were similar. According to the report by Dong et al. (13), the HA protein of influenza virus was assembled as efficiently into the envelope of RSV as the homologous RSV spike. However, also in this case it is unclear whether the densities of these proteins at the cell surface were similar. Furthermore, the incorporation was assayed in a vaccinia virus T7-driven RSV assembly system, which apparently yielded a high expression level for these proteins. The obtained differences in the relative efficiencies of incorporation of SFV spikes and TRΔ2 under the low and high synthesis levels reported here raise a note of caution concerning the interpretation of results obtained under high expression levels. Interestingly however, the cellular proteins β_2-microglobulin and human lymphocyte antigen (HLA) DR were found to outnumber gp120 in purified human immunodeficiency virus types 1 and 2 and simian immunodeficiency virus particles produced from wild type-infected cells (2). Clearly, it would be interesting to test how efficiently HLA-DR or the influenza virus and RSV spike proteins are incorporated into extracellular particles in our M-MuLV assembly system.

The basis for the differential incorporation of M-MuLV and SFV spike proteins (or TRΔ2) is at present unclear and can only be speculated upon. M-MuLV spike proteins were efficiently assembled into extracellular M-MuLV particles when expressed at a relatively low density at the plasma membrane, whereas the efficient inclusion of heterologous membrane proteins was strictly dependent on the high-level expression of these proteins at the cell surface. The high amounts of SFV spike proteins in the particles produced from SFV-C/$Pr65^{gag}$- and SFV-(E2Y399K)-cotransfected cells imply that the overall three-dimensional structure of the SFV spike complex was not incompatible with efficient incorporation. Therefore, the differential incorporation of the M-MuLV and SFV spike proteins at the low expression level can be taken to indicate that homologous and heterologous membrane proteins are incorporated into the M-MuLV envelope via two distinct pathways. The simplest explanation for the preferential incorporation of M-MuLV spikes is the concept that specific core-spike interactions facilitate the incorporation of homologous spike proteins into particles. This assumption is supported by reports that deletions or insertions in the cytoplasmic domain of the M-MuLV spike can reduce incorporation of the mutant spike proteins into virions (22, 23). Incorporation of a heterologous protein into the M-MuLV envelope could occur nonspecifically and be governed by factors such as (i) the density of the protein at the cell surface, (ii) the compatibility of the three-dimensional structure of the protein, and (iii) whether there are interactions between the protein and endogenous cellular components which would restrict the mobility of the former in the membrane and hence interfere with its access to the budding site. That this third point could be important is

suggested by an observation that the amount of influenza virus HA in RSV particles was markedly increased if cells producing virions were treated with exogenous neuraminidase, a treatment that presumably freed HA from other plasma membrane proteins (13). Although in this present study the relative mobilities of M-MuLV and SFV spike proteins in the plasma membrane were not determined, it is unlikely that the different incorporation efficiencies of the proteins could be solely due to differences in their mobilities. Both M-MuLV and SFV spike proteins are alien to BHK cells, and thus these proteins would be expected to lack interactions with endogenous host components. Indeed, previous experiments have indicated that the SFV spike complex is not subjected to rapid endocytosis in BHK cells (62). Although BHK cells express a receptor for SFV (55), it is unlikely that interactions with this receptor would have caused the observed inefficient incorporation of SFV spike proteins at the low expression level, because previous studies have indicated that the unprocessed p62-spike complex used in the experiments is impaired in receptor binding (45). However, to conclusively settle whether putative core-spike interactions were the sole factor influencing the differential incorporation of homologous and heterologous proteins observed here, biochemical binding assays as well as direct mobility measurements are required.

ACKNOWLEDGMENTS

We are grateful to Georg Schmidt for providing the anti-p30 antiserum, to Harm Snippe for providing the monoclonal anti-E1 antibody, to Irene Greiser-Wilke for providing the monoclonal anti-C antibody, and to Thomas Ebel for providing the monoclonal anti-TR antibody. We also thank Stephen Goff for providing the pNCA plasmid, Kristina Wallengren for providing the pSFV1-Pr80^{env} plasmid, Peter Liljeström for providing the pSFV-(E2Y399K) plasmid, Bernd-Uwe Barth for providing the SFV1-p62*E1 plasmid, Mona-Lisa Strand for her contributions to the construction of the various plasmids used in the study, Lars Melin for his expert advice concerning the use of PCR, and Roger Hewson and Joan Smyth for critically reading the manuscript.

This work was supported by the Swedish Natural Science Research Council (B-BU 09353-306) and the Swedish Cancer Society (3277-B93-02XBB).

REFERENCES

1. **Aliperti, G., and M. J. Schlesinger.** 1978. Evidence for an autoprotease activity of Sindbis virus capsid protein. Virology **90**:366–369.
2. **Arthur, L., J. Bess, R. Sowder, R. Benveniste, D. Mann, J.-C. Chermann, and L. Henderson.** 1992. Cellular proteins bound to immunodeficiency viruses: implications for pathogenesis and vaccines. Science **258**:1935–1938.
3. **Barth, B.-U., and H. Garoff.** Unpublished data.
4. **Berglund, P., M. Sjöberg, H. Garoff, G. Atkins, B. Sheahan, and P. Liljeström.** 1993. Semliki Forest virus expression system: production of conditionally infectious recombinant particles. Bio/Technology **11**:916–920.
5. **Boere, W. A. M., T. Harmsen, J. Vinje, B. J. Benaissa-Trouw, C. A. Kraaijeeveld, and H. Snippe.** 1984. Identification of distinct antigenic determinants on Semliki Forest virus by using monoclonal antibodies with different antiviral activities. J. Virol. **52**:575–582.
6. **Burns, J., T. Friedman, W. Driever, M. Burrascano, and J.-K. Yee.** 1993. Vesicular stomatitis virus G glycoprotein pseudotyped retroviral vextors: concentration to very high titer and efficient gene transfer into mammalian and nonmammalian cells. Proc. Natl. Acad. Sci. USA **90**:8033–8037.
7. **Calafat, J., H. Janssen, P. Demant, J. Hilgers, and J. Zavada.** 1983. Specific selection of host cell glycoproteins during assembly of murine leukemia virus and vesicular stomatitis virus: presence of Thy-1 glycoprotein and absence of H-2, Pgp-1 and T-200 glycoproteins on the envelopes of these virus particles. J. Gen. Virol. **64**:1241–1253.
8. **Choi, H.-K., L. Tong, W. Minor, P. Dumas, U. Boege, M. G. Rossmann, and G. Wengler.** 1991. Structure of Sindbis virus core protein reveals a chymotrypsin-like serine proteinase and the organization of the virion. Nature (London) **354**:37–43.
9. **Colicelli, J., and S. P. Goff.** 1988. Sequence and spacing requirements of a retrovirus integration site. J. Mol. Biol. **199**:47–59.
10. **Collawn, J. F., M. Stangel, L. A. Kuhn, V. Esekogwu, S. Jing, I. S. Trowbridge, and J. A. Tainer.** 1990. Transferrin receptor internalization sequence YXRF implicates a tight turn as the structural recognition motif for endocytosis. Cell **63**:1061–1072.
11. **de Curtis, I., and K. Simons.** 1988. Dissection of Semliki Forest virus glycoprotein delivery from the trans-Golgi network to the cell surface in permeabilized BHK cells. Proc. Natl. Acad. Sci. USA **85**:8052–8056.
12. **Delchambre, M., D. Gheysen, D. Thines, C. Thiriart, E. Jacobs, E. Verdin, M. Horth, A. Burny, and F. Bex.** 1989. The GAG precursor of simian immunodeficiency virus assembles into virus-like particles. EMBO J. **8**:2653–2660.
13. **Dong, J., M. Roth, and E. Hunter.** 1992. A chimeric avian retrovirus containing the influenza virus hemagglutinin gene has an expanded host range. J. Virol. **66**:7374–7382.
14. **Dorfman, T., F. Mammano, W. A. Haseltine, and H. G. Göttlinger.** 1994. Role of the matrix protein in the virion association of the human immunodeficiency virus type 1 envelope glycoprotein. J. Virol. **68**:1689–1696.
15. **Dougherty, J., R. Wisniewski, S. Yang, B. W. Rhode, and H. Temin.** 1989. New retrovirus helper cells with almost no nucleotide sequence homology to retrovirus vectors. J. Virol. **63**:3209–3212.
16. **Dunphy, W., and J. Rothman.** 1985. Compartmental organization of the Golgi stack. Cell **42**:13–21.
17. **Emi, N., T. Friedman, and J.-K. Yee.** 1991. Pseudotype formation of murine leukemia virus with the G protein of vesicular stomatitis virus. J. Virol. **65**:1202–1207.
18. **Feng, Y.-X., H. Yuan, A. Rein, and J. Levin.** 1992. Bipartite signal for read-through suppression in murine leukemia virus mRNA: an eight-nucleotide purine-rich sequence immediately downstream of the *gag* termination codon followed by an RNA pseudoknot. J. Virol. **66**:5127–5132.
19. **Garoff, H., D. Huylebroeck, A. Robinson, U. Tillman, and P. Liljeström.** 1990. The signal sequence of the p62 protein of Semliki Forest virus is involved in initiation but not in completing chain translocation. J. Cell Biol. **111**:867–876.
20. **Garoff, H., K. Simons, and B. Dobberstein.** 1978. Assembly of Semliki Forest virus membrane glycoproteins in the membrane of the endoplasmic reticulum in vitro. J. Mol. Biol. **124**:587–600.
21. **Gheysen, D., E. Jacobs, F. de Foresta, C. Thiriart, M. Francotte, D. Thines, and M. De Wilde.** 1989. Assembly and release of HIV-1 precursor Pr55^{gag} virus-like particles from recombinant baculovirus-infected cells. Cell **59**:103–112.
22. **Granowitz, C., J. Colicelli, and S. P. Goff.** 1991. Analysis of mutations in the envelope gene of Moloney murine leukemia virus: separation of infectivity from superinfection resistance. Virology **183**:546–554.
23. **Gray, K., and M. Roth.** 1993. Mutational analysis of the envelope gene of Moloney murine leukemia virus. J. Virol. **67**:3489–3496.
24. **Greiser-Wilke, I., V. Moennig, O.-R. Kaaden, and L. T. M. Figueiredo.** 1989. Most alphaviruses share a conserved epitopic region on their nucleocapsid protein. J. Gen. Virol. **70**:743–748.
25. **Hallenberger, S., V. Bosch, H. Angliker, E. Shaw, H.-D. Klenk, and W. Garten.** 1992. Inhibition of furin-mediated cleavage activation of HIV-1 glycoprotein gp160. Nature (London) **360**:358–361.
26. **Hansen, M., L. Jelinek, R. Jones, J. Stegeman-Olsen, and E. Barklis.** 1993. Assembly and composition of intracellular particles formed by Moloney murine leukemia virus. J. Virol. **67**:5163–5174.
27. **Hansen, M., L. Jelinek, S. Whiting, and E. Barklis.** 1990. Transport and assembly of *gag* proteins into Moloney murine leukemia virus. J. Virol. **64**:5306–5316.
28. **Horton, R., H. Hunt, S. Ho, J. Pullen, and L. Pease.** 1989. Engineering hybrid genes without the use of restriction enzymes: gene splicing by overlap extension. Gene **77**:61–68.
29. **Hoxie, J., T. Fotzharris, P. Youngbar, D. Matthews, J. Rackowski,**

and S. Radka. 1987. Nonrandom association of cellular antigens with HTLV-III virions. Hum. Immunol. **18:**39–52.
30. **Hsu, H.-W., P. Schwartzberg, and S. Goff.** 1985. Point mutations in the p30 domain of the gag gene of Moloney murine leukemia virus. Virology **142:**211–214.
31. **Kiilunen, T., and H. Garoff.** Unpublished data.
32. **Landau, N., and D. Littman.** 1992. Packaging system for rapid production of murine leukemia virus vectors with variable tropism. J. Virol. **66:**5110–5113.
33. **Landau, N., K. Page, and D. Littman.** 1991. Pseudotyping with human T-cell leukemia virus type I broadens the human immunodeficiency virus host range. J. Virol. **65:**162–169.
34. **Lando, Z., P. Sarin, M. Megson, W. C. Greene, T. A. Waldman, R. C. Gallo, and S. Broder.** 1983. Association of human T-cell leukaemia/lymphoma virus with the Tac antigen marker for the human T-cell growth factor receptor. Nature (London) **305:**733–736.
35. **Liljeström, P., and H. Garoff.** 1991. A new generation of animal cell expression vectors based on the Semliki Forest virus replicon. Bio/Technology **9:**1356–1361.
36. **Liljeström, P., and H. Garoff.** 1991. Internally located cleavable signal sequences direct the formation of Semliki Forest virus membrane proteins from a polyprotein precursor. J. Virol. **65:**147–154.
37. **Liljeström, P., S. Lusa, D. Huylebroeck, and H. Garoff.** 1991. In vitro mutagenesis of a full-length cDNA clone of Semliki Forest virus: the 6,000-molecular-weight membrane protein modulates virus release. J. Virol. **65:**4107–4113.
38. **Luciw, P. A., and N. J. Leung.** 1992. Mechanisms of retrovirus replication, p. 159–298. *In* J. A. Levy (ed.), The Retroviridae, vol. 1. Plenum Press, New York.
39. **Melançon, P., and H. Garoff.** 1987. Processing of the Semliki Forest virus structural polyprotein: role of the capsid protease. J. Virol. **61:**1301–1309.
40. **Neefjes, J. J., T. Henegveld, O. Tol, and H. L. Ploegh.** 1990. Intracellular interactions of transferrin and its receptor during biosynthesis. J. Cell Biol. **111:**1383–1392.
41. **Ng, V., T. G. Wood, and R. B. Arlinghaus.** 1982. Processing of the env gene products of Moloney murine leukemis virus. J. Gen. Virol. **59:**329–343.
42. **Peränen, J., K. Takkinen, N. Kalkkinen, and L. Kääriäinen.** 1988. Semliki Forest virus-specific non-structural protein nsP3 is a phosphoprotein. J. Gen. Virol. **69:**2165–2178.
43. **Rhee, S., and E. Hunter.** 1990. A single amino acid substitution within the matrix protein of type D retrovirus converts its morphogenesis to that of a type C retrovirus. Cell **63:**77–86.
44. **Rhee, S. S., H. Hui, and E. Hunter.** 1990. Preassembled capsids of type D retroviruses contain a signal sufficient for targeting specifically to the plasma membrane. J. Virol. **64:**3844–3852.
45. **Salminen, A., J. M. Wahlberg, M. Lobigs, P. Liljeström, and H. Garoff.** 1992. Membrane fusion process of Semliki Forest virus. II. Cleavage dependent reorganization of the spike protein complex controls virus entry. J. Cell Biol. **116:**349–357.
46. **Schwartzberg, P., J. Colicelli, M. Gordon, and S. Goff.** 1984. Mutations in the *gag* gene of Moloney murine leukemia virus: effects on production of virions and reverse transcriptase. J. Virol. **49:**918–924.
47. **Shields, A., O. N. Witte, E. Rothenberg, and D. Baltimore.** 1978. High frequency of aberrant expression of Moloney murine leukemia virus in clonal infections. Cell **14:**601–609.
48. **Sjöberg, M., M. Suomalainen, and H. Garoff.** Unpublished data.
49. **Smith, A., N. Srinivasakumar, M.-L. Hammarskjold, and D. Rekosh.** 1993. Requirements for incorporation of $Pr160^{gag\text{-}pol}$ from human immunodeficiency virus type 1 into virus-like particles. J. Virol. **67:**2266–2275.
50. **Su, T.-Z., and M. R. El-Gewely.** 1988. A multisite-directed mutagenesis using T7 DNA polymerase: application for reconstructing a mammalian gene. Gene **69:**81–89.
51. **Suomalainen, M., M. Baron, and H. Garoff.** 1990. The E2 signal sequence of rubella virus remains part of the capsid protein and confers membrane association in vitro. J. Virol. **64:**5500–5509.
52. **Suomalainen, M., P. Liljeström, and H. Garoff.** 1992. Spike protein-nucleocapsid interactions drive the budding of alphaviruses. J. Virol. **66:**4737–4747.
53. **Vile, R., T. Schulz, O. Danos, M. Collins, and R. Weiss.** 1991. A murine cell line producing HTLV-I pseudotype virions carrying a selectable marker gene. Virology **180:**420–424.
54. **Wahlberg, J. M., W. A. Boere, and H. Garoff.** 1989. The heterodimeric association between the membrane proteins of Semliki Forest virus changes its sensitivity to mildly acidic pH during virus maturation. J. Virol. **63:**4991–4997.
55. **Wang, K.-S., R. J. Kuhn, E. G. Strauss, S. Ou, and J. H. Strauss.** 1992. High-affinity laminin receptor is a receptor for Sindbis virus in mammalian cells. J. Virol. **66:**4992–5001.
56. **Wilson, C., M. S. Reitz, H. Okayama, and M. V. Eiden.** 1989. Formation of infectious hybrid virions with gibbon ape leukemia virus and human T-cell leukemia virus retroviral envelope glycoproteins and the *gag* and *pol* proteins of Moloney murine leukemia virus. J. Virol. **63:**2374–2378.
57. **Witte, O., A. Tsukamoto-Adey, and I. L. Weissman.** 1977. Cellular maturation of oncornavirus glycoproteins: topological arrangement of precursor and product forms in cellular membranes. Virology **76:**539–553.
58. **Yon, J., and M. Friend.** 1989. Precise gene fusion by PCR. Nucleic Acids Res. **17:**4895.
59. **Young, J., P. Bates, K. Willert, and H. Varmus.** 1990. Efficient incorporation of human CD4 protein into avian leukosis virus particles. Science **250:**1421–1423.
60. **Yu, X., X. Yuan, Z. Matsuda, T.-H. Lee, and M. Essex.** 1992. The matrix protein of human immunodeficiency virus type 1 is required for incorporation of viral envelope protein into mature virions. J. Virol. **66:**4966–4971.
61. **Zavada, J.** 1982. The pseudotypic paradox. J. Gen. Virol. **63:**15–24.
62. **Zhao, H., and H. Garoff.** 1992. Role of cell surface spikes in alphavirus budding. J. Virol. **66:**7089–7095.
63. **Zhao, H., B. Lindqvist, H. Garoff, A. Salminen, C.-H. von Bonsdorff, and P. Liljeström.** A tyrosine-based motif in the cytoplasmic domain of the alphavirus envelope protein is essential for budding. Submitted for publication.
64. **Ziemiecki, A., H. Garoff, and K. Simons.** 1980. Formation of the Semliki Forest virus membrane glycoprotein complexes in the infected cell. J. Gen. Virol. **50:**111–123.